ACS OMEGA

http://pubs.acs.org/journal/acsodf

Article

Electromagnetic Characterization of a Multiwalled Carbon Nanotubes−Silver Nanoparticles-Reinforced Polyvinyl Alcohol Hybrid Nanocomposite in X-Band Frequency

Yusliza Yusof,* Seyedehmaryam Moosavi, Mohd Rafie Johan,* Irfan Anjum Badruddin, Yasmin Abdul Wahab, Nor Aliya Hamizi, Marlinda Ab Rahman, Sarfaraz Kamangar, and T. M. Yunus Khan

Cite This: *ACS Omega* 2021, 6, 4184−4191

Read Online

ACCESS | Metrics & More | Article Recommendations

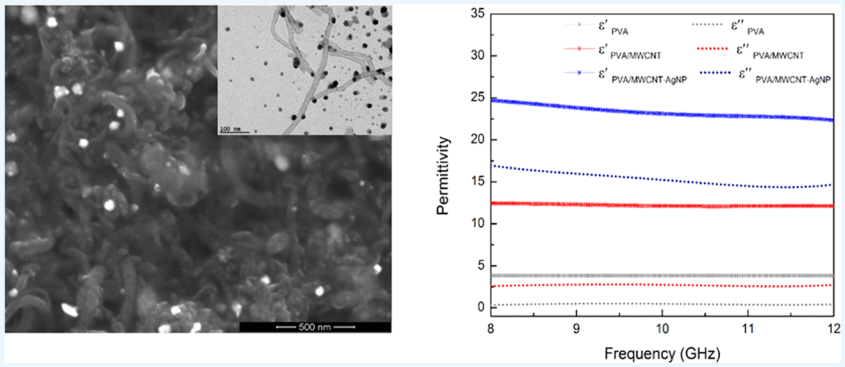

ABSTRACT: This study presents the electromagnetic (EM) characterization of a multiwalled carbon nanotubes (MWCNT)−silver nanoparticles (AgNP)-reinforced poly(vinyl alcohol) (PVA) hybrid nanocomposite fabricated via the solution mixing technique. Primarily, the structure and morphological properties of the PVA/MWCNT−AgNP hybrid nanocomposite are confirmed by X-ray diffraction (XRD) and field emission scanning electron microscopy (FESEM). The complex permittivity (ε^*) and permeability (μ^*), as well as the electromagnetic scattering parameters are measured using a PNA network analyzer equipped with X-band waveguide. The results showed an enhanced permittivity ($\varepsilon' \approx 25$) value of the hybrid nanocomposite in the frequency range of 8−12 GHz. However, the permeability decreased to almost zero ($\mu' \approx 0.4$) since the inclusion of AgNP with an average particle size of 40 nm is not susceptible to magnetization and causes higher magnetic losses ($\tan \delta_\mu$) than dielectric losses ($\tan \delta_\varepsilon$). Remarkably, the hybrid nanocomposite reduced transmission of electromagnetic (EM) wave by nearly 60% in comparison to PVA/MWCNT. This is attributed to the enhanced absorption and reflection at the nanotubes, and metal−dielectric interfaces have induced multiple internal reflections owing to the porous structure of the nanocomposite. The prospect of the PVA/MWCNT−AgNP hybrid nanocomposite is favorable as a thin absorbing material for EM shielding applications.

1. INTRODUCTION

The proliferation of electronic devices and telecommunications such as mobile phones, radio and television antennas, radar transmitters, as well as microwave ovens has caused a major concern in electromagnetic interference (EMI). Therefore, EMI shielding materials are needed to protect some devices that are susceptible to the interference from passing a limited boundary whether by reflection or absorption. Typical materials used for conventional electromagnetic shielding have high electrical conductivity of metal sheets or meshes by providing total reflection at the surface of the materials via the Faraday cage effect.[1,2] However, metals have some drawbacks due to poor mechanical flexibility, high weight density, and susceptible to corrosion. Unlikely, polymer-based composites are more reliable with lightweight, low cost, and easy shaping property for specific designs in EMI applications.

Most polymers are transparent to electromagnetic waves due to their intrinsic insulating properties that require further modifications. In this case, reflectivity and absorption characteristics of electromagnetic waves in polymeric materials

Received: October 5, 2020
Accepted: January 25, 2021
Published: February 3, 2021

https://dx.doi.org/10.1021/acsomega.0c04864
ACS Omega 2021, 6, 4184−4191

can be tuned by the reinforcement of conductive nanoscale fillers to manipulate the outstanding electrical conductivity and superior dielectric/magnetic properties.[2] Greater changes in electromagnetic properties are expected as particle sizes of the fillers decreased to the nanoscale due to relatively low density and high specific surface area.[3] In recent years, nanomaterials have received significant attention as amongst the promising materials that can cut off those EM radiations in a wide range of applications. Particularly, carbon nanotubes (CNT) are the one-dimensional nanomaterials that possess excellent electrical conductivity and favorable for EM wave absorption.[4−7] In the literature, CNT-based polymer nanocomposites have been stated to exhibit a parallel trend of dielectric permittivity and dielectric loss due to their high surface area-to-volume ratio.[8,9] Another study has reported a low frequency dependence of dielectric permittivity in polymer nanocomposites having a CNT content of less than 5 wt %.[10]

Alternatively, the integration of CNT and metal particles can impart further unique characteristics including catalytic, optical, electronic, and magnetic properties. CNT can be the most favorable platform for making contacts with metallic nanoparticles due to their surface reactivity.[11] The decoration of CNT with noble metals like silver nanoparticles (AgNP) has been reported to show a significant rise in electrical conductivity at a lower percolation threshold.[12−15] The nanoparticles are expected to cause high energy losses, which enables them to absorb the incident wave energy and dissipate it as heat. Thus, a few studies were focused on lowering dielectric losses ascribed to the high electrical conduction triggered by AgNP as the Coulomb blockade effect.[16,17] In addition, the incorporation of CNT−AgNP in dielectric media has been reported for microwave absorption due to high interfacial polarization and multiple scattering at the metal−dielectric interfaces.[18−20] However, the use of both fillers for broad bandwidth of thin absorbing materials in gigahertz frequency is still limited.

Therefore, this work aims to evaluate the electromagnetic properties of a multiwalled carbon nanotubes−silver nanoparticles (MWCNT−AgNP)-reinforced poly(vinyl alcohol) (PVA) hybrid nanocomposite. To the best of our knowledge, it has yet been reported elsewhere and, to a lesser extent, relies on the interaction of the materials with the electromagnetic field. PVA is well known as a polar polymer and a good dielectric host for encapsulating nanotubes due to its high content of hydroxyl groups. Hydroxyl groups are strong dipoles that can align with electric field to increase polarization in nanocomposites.[21] However, multiwalled carbon nanotubes (MWCNT) were selected as they offer exciting electrical and electronic properties due to multiwalled configurations and large diameters, which can favor low ohmic contact at the outermost nanotube walls.[22] In light of this work, the performance of PVA/MWCNT−AgNP hybrid nanocomposite is evaluated in comparison to merely PVA/MWCNT and pure PVA. It covers the structure and morphological analysis, while the electromagnetic analysis includes complex permittivity and permeability, as well as scattering parameters in X-band frequency ranging from 8 to 12 GHz.

2. EXPERIMENTAL SECTION

2.1. Materials. The materials used in this work include PVA powder (M_w = 31 000−50 000 g/mol, 98−99% hydrolyzed), which was purchased from Sigma-Aldrich, and MWCNT (purity > 90%) with a diameter of 4−12 nm and length of 10−30 μm, which were purchased from Nanoshel U.K. Limited. Hydrogen peroxide (H_2O_2, 30%) and nitric acid (HNO_3, 65%) supplied by R&M Chemicals were used for surface functionalization of the MWCNT. Silver nitrate ($AgNO_3$, 0.1 mol/L) and *N*,*N*-dimethylformamide (DMF, 73.1 g/mol) also supplied by R&M Chemicals were chosen as the Ag precursor and reducing agent, respectively. Sodium dodecyl sulfate (SDS) obtained from R&M Marketing Essex was used as surfactants to provide good dispersion of the nanoparticles.

2.2. Preparation of PVA Nanocomposites. First, 500 mg of MWCNT was functionalized using mild ultrasonication treatment at room temperature in 100 mL of nitric acid (HNO_3, 65%) for 1 h and washed with deionized water several times to make the pH value neutral. Then, the solvent was changed to hydrogen peroxide (H_2O_2, 30%) with the same treatment, followed by filtration and drying processes to remove all of the solvents. Then, the hybrid MWCNT−AgNP was synthesized through a single step by reducing silver ions (Ag^+) from its precursor in a dispersion of MWCNT. The functionalized MWCNT (420 mg) and SDS (160 mg) were dispersed in 140 mL of DMF. The mixed solution was sonicated in an ultrasonic bath for 30 min and slowly heated to 80 °C; then, 140 mL of aqueous $AgNO_3$ (0.1 mol/L) was added into the solution at a flow rate of 60 mL/min. The hot solution was stirred continuously for an hour and left to cool overnight at room temperature. The precipitation of the final product was filtered; washed with ethanol, water, and acetone several times; and then dried at 60 °C for 24 h.

Then, the nanocomposites were prepared by the solution mixing and casting technique. The same weight of functionalized MWCNT without adding $AgNO_3$ and MWCNT−AgNP hybrid was dispersed in 100 mL of distilled water in a separate beaker assisted with 160 mg of SDS as the surfactant upon ultrasonication within 30 min. Subsequently, 5000 mg of PVA powder was added into both sonicated solutions and slowly heated to 85 °C with continuous stirring at 750 rpm and held for 1 h to ensure complete solubility and homogeneity of the PVA solutions. The obtained viscous solutions were immediately poured into glass Petri dishes and dried at room temperature for 48 h. On average, the thickness of the final nanocomposite films was 0.34 mm. Finally, the samples were kept dry in a vacuum desiccator for 3 days before characterization.

2.3. Characterization. An X-ray diffractometer (XRD, PANalytical Empyrean) was used to identify the crystallographic structure of samples using Cu Kα radiation of λ = 1.54 060 nm. The data were collected by scanning the diffraction angle in the range of 2θ = 10−80°. Field emission scanning electron microscopy (FESEM, FEI QUANTA 450 FEG) was carried out to observe the microstructures of MWCNT and AgNP embedded in the matrix PVA. The samples were mounted on a special holder before inserting into the high-vacuum part of the microscope through an exchange chamber that was fixed on a movable stage. It was operated at an accelerating voltage of 5 kV. Transmission electron microscopy (TEM, JEOL-JEM 2100-F) was employed to observe the internal structure and particle size of the as-synthesized MWCNT−AgNP. It was subjected to ultrasonication in deionized water for 20 min. Then, the suspension was dropped onto formvar/carbon-coated copper 300 mesh grids with a diameter of 3.05 mm upon examination.

https://dx.doi.org/10.1021/acsomega.0c04864
ACS Omega 2021, 6, 4184−4191

Electromagnetic parameter measurements for the samples were carried out using an N5227A PNA network analyzer (Keysight Technologies). The PNA comes with two ports connected to an X-band waveguide WR-90 that has four holes fixed at both ends The nanocomposite sheets were enclosed on a sample launcher of a rectangular waveguide with the dimension of 23 × 10 mm^2, as shown in Figure 1. The PNA

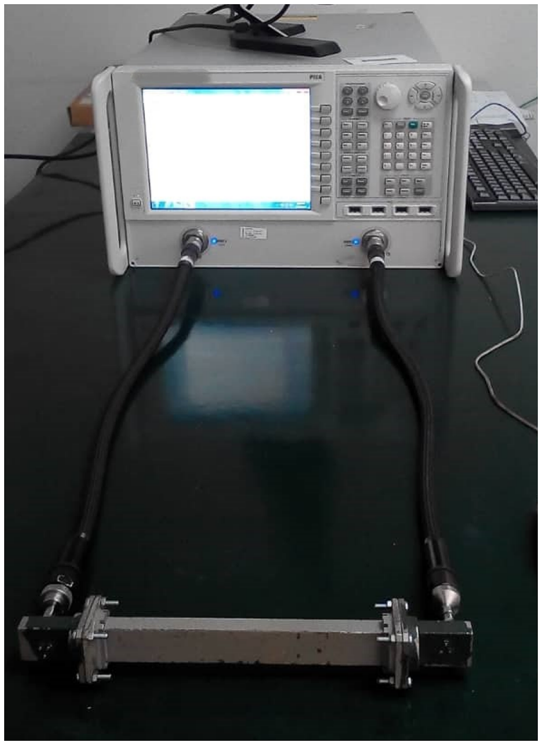

Figure 1. Setup of X-band waveguide connected with a PNA network analyzer.

was calibrated based on the thru-reflect-line (TRL) calibration technique for 201 frequency points. The calibration standard canceled out the effect of cables and connectors as well as imperfections of the test setup by testing the sample using an ideal reflector and absorber.

The test allows simultaneous measurement of electrical network scattering parameters or S-parameters (S_{ii}) between the two ports using algorithm software 85071E to perform the conversion of complex permittivity ($\varepsilon^* = \varepsilon' - j\varepsilon''$) and complex permeability ($\mu^* = \mu' - i\mu''$). The TRL setup directly measures the reflected power signal (S_{11}) and transmitted power signal (S_{12}) over the given frequency range from port 1 to port 2 and vice versa. Thus, the electromagnetic characterization for transmission (T), reflection (R), and absorption (A) can be simply expressed by the following equations

$$T = |S_{12}|^2 = (|S_{21}|^2) \quad (1)$$

$$R = |S_{11}|^2 = (|S_{22}|^2) \quad (2)$$

$$A = 1 - R - T \quad (3)$$

3. RESULTS AND DISCUSSION

3.1. XRD Analysis. XRD patterns in Figure 2 show the crystalline structure and chemical composition of the PVA/

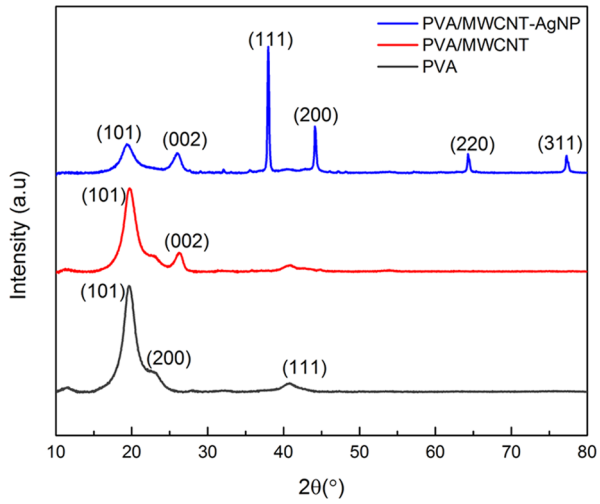

Figure 2. XRD patterns of PVA with MWCNT and MWCNT−AgNP hybrid nanocomposites.

MWCNT−AgNP nanocomposite compared to pure PVA and PVA/MWCNT. It depicts that PVA formerly exhibits a broad diffraction peak at 2θ = 19.2° and a shoulder at 2θ = 23.0°, which correspond to the reflection planes (101) and (200) from a monoclinic unit cell.[23] However, the PVA/MWCNT exhibits a new peak at 2θ = 26.3°, which corresponds to a typical (002) plane of the MWCNT. The interplanar distance, d_{hkl}, for the (002) plane of MWCNT is 0.341 nm. PVA/MWCNT−AgNP shows the presence of polycrystalline AgNP in the nanocomposite with more intense peaks at 2θ = 38.1, 44.3, 64.5, and 77.4° assigned to the reflections of Ag planes (111), (200), (220), and (311), respectively.[24] The d_{hkl} values of the Ag planes possessing a face-centered cubic [FCC] structure determined by Bragg's law are 0.236, 0.204, 0.144, and 0.123 nm. The average lattice constant, a, is determined to be 0.410 nm, which is in good agreement with the standard value [Silver file no. 01-087-0717]. However, the width and intensity peak at 2θ = 19.2° correspond to the decreases of matrix PVA in the presence of MWCNT−AgNP triggering the increase of crystallite size in accordance with the Scherrer formula.[25] The crystallization of PVA is favored due to the high hydrolysis degree of the polymer containing hydroxyl groups, which could also result in more intermolecular interactions with both the fillers.

3.2. FESEM Analysis. The FESEM image of the PVA/MWCNT−AgNP nanocomposite is shown in Figure 3. It shows a filmlike morphology of MWCNT−AgNP embedded in the PVA matrix. The structure of MWCNT is more kinked and distributed with high irregular interfaces, while the addition of AgNP could reduce van der Waals forces and prevent agglomeration of the nanotubes.[13] AgNP can be seen as bright spherical spots with an average particle size of 40 nm and were grafted on the surfaces of MWCNT. The inset of this figure shows the transmission electron microscopy (TEM) image depicting the attachment of a few AgNP onto the MWCNT surfaces while some nanoparticles are only distributed around the nanotubes. However, the interconnected network of MWCNT−AgNP still provides favorable interactions between the matrix and the fillers. The MWCNT serves as the conducting bridges when in contact with the AgNP that could reduce the potential barrier of two localized states by forming charge transfer complexes (CTC) in

https://dx.doi.org/10.1021/acsomega.0c04864
ACS Omega 2021, 6, 4184−4191

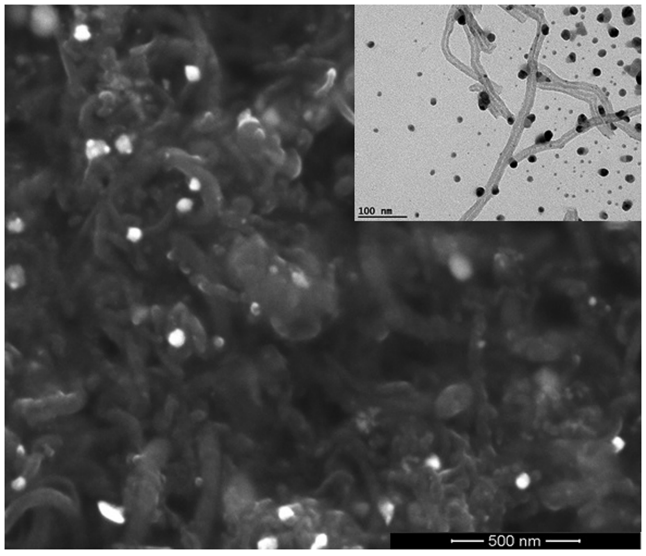

Figure 3. FESEM image of the PVA/MWCNT−AgNP hybrid nanocomposite. The inset is the TEM image of the MWCNT−AgNP.

amorphous regions of the semicrystalline polymer matrix.[26,27] The difference in electrical conductivity between MWCNT and AgNP also creates high interfacial polarization in the hybrid nanocomposite. The interfacial polarization occurs when the motion of moving charge is impeded at the interfaces of a material. There could be multiple interfacial polarizations due to the large specific areas of both MWCNT and AgNP, which can lead to an increase in dielectric permittivity.

3.3. Complex Permittivity and Permeability Analysis.

The basic parameters in determining the electromagnetic properties of the samples are related to the behavior of their complex permittivity and complex permeability. Figure 4a depicts the variation of complex permittivity as a function of frequency for PVA, PVA/MWCNT, and MWNT−AgNP hybrid nanocomposites measured in the X-band frequency. The complex permittivity comprises the real part ε' and the imaginary part ε'', which represent storage of electric energy (also known as dielectric constant) and energy loss, respectively. Initially, PVA shows a constant ε' value of 4.5 as the frequency increases from 8 to 12 GHz. The incorporation of MWCNT increased the ε' value of PVA to 12, yet it tends to become constant over the applied frequency. It shows that the displacement or polarizations of charge carriers at a low MWCNT content have remained unchanged in the X-band frequency because the charges locally bound in atoms, molecules, or defect structures rearrange their position in response to the electromagnetic field.[28]

The incorporation of MWCNT−AgNP in PVA has increased the maximum ε' value to nearly 25 with a small decline as the frequency increases from 8 to 12 GHz. This finding is higher than that reported for Ag/CNT loaded in paraffin wax, in which the ε' value is lower than 10 in the same frequency range.[20] It could be because the paraffin wax is not a good dielectric medium to trigger strong polarization of Ag/CNT within the hydrocarbon molecules. In contrast, the inclusion of MWCNT−AgNP induced a larger magnitude of polarization in the PVA composite due to strong permanent dipoles created by the high content of hydroxyl groups in the polymer chain.[21] The interfacial polarization also increases with the existence of free mobile electrons coming from the Ag

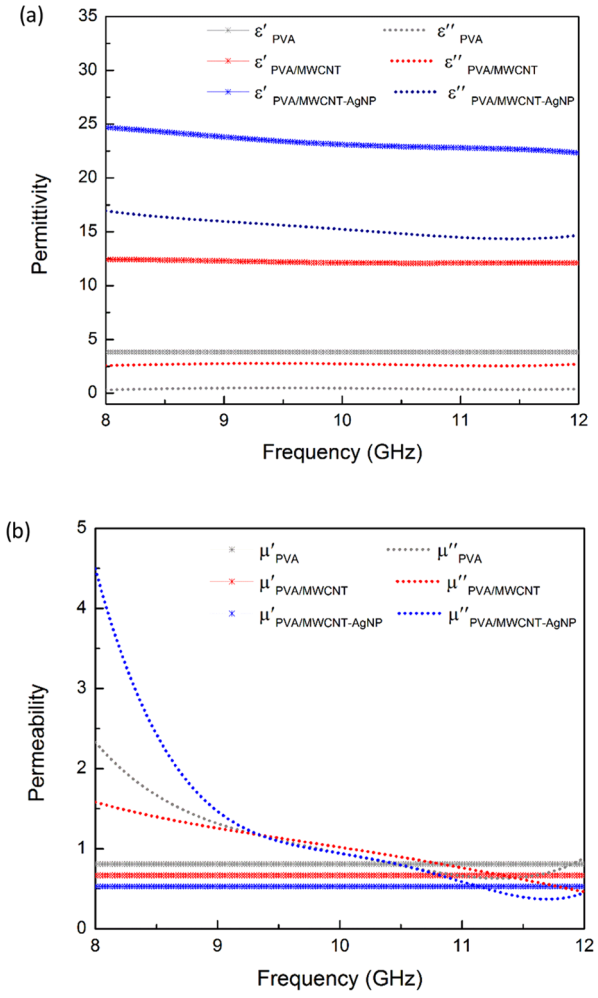

Figure 4. Variation of (a) complex permittivity (ε', ε'') and (b) complex permeability (μ', μ'') versus frequency in PVA nanocomposites.

particles, and the backbone of MWCNT is impeded at the interfaces between the conducting and insulating regions.[29] However, the ε'' value of the hybrid nanocomposite decreased gradually with an increase in frequency, showing a greater loss prompted by the MWCNT−AgNP to dissipate the EM energy.

Figure 4b depicts complex permeability also composed of the real part μ' and the imaginary part μ'', which denotes the storage of magnetic energy and loss, respectively. The trend of μ' for PVA and PVA/MWCNT is primarily independent of frequency in the range of 8−12 GHz, which lie constantly at 0.8 and 0.7, respectively, while PVA/MWCNT−AgNP hybrid nanocomposite remains constant at the smallest μ' value of 0.4. As the μ' value is much lower than 1, it indicates that the hybrid nanocomposite exhibits a weaker magnetic response to an external magnetic field due to less magnetization by the presence of AgNP. This is expected since MWCNT and AgNP are themselves nonmagnetic materials with permeability close to 1 ($\mu' \approx 1$). In contrast, the magnetic loss μ'' trends for PVA and PVA/MWCNT decrease gradually with an increase in the applied frequency. However, the μ'' value of the PVA/MWCNT−AgNP hybrid nanocomposite decreases rapidly from 4.5 to 0.4 as the frequency increases, where the inflection points are observed at 9 and 11.5 GHz. The magnetic losses arise from alternating hysteresis losses and eddy current losses caused repulsive forces with the applied magnetic fields as

https://dx.doi.org/10.1021/acsomega.0c04864
ACS Omega 2021, 6, 4184−4191

induced by good electrical conduction of the material.[30] Figure 5 shows that the ac conductivity, σ_{ac}, values of PVA and PVA/MWCNT are found to be low and less dependent on frequency, while that of the PVA/MWCNT−AgNP hybrid nanocomposite slightly varies with frequency as the conductivity increases from 7.5 to 10 S/m. This is ascribed to the tunneling effect when the electrons gain a higher energy as the frequency increases at the adjacent conducting particles between MWCNT and AgNP.[31,32]

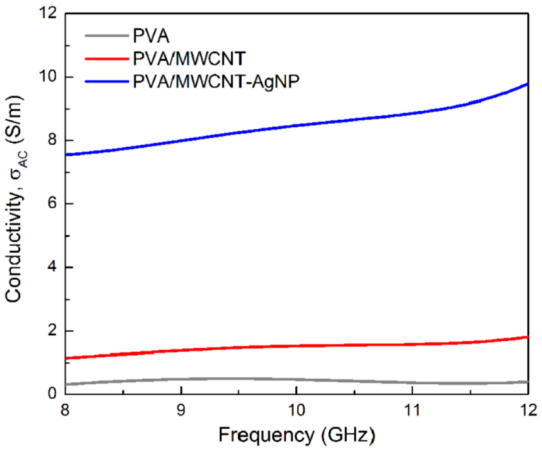

Figure 5. Ac conductivity versus frequency in PVA nanocomposites.

The inherent dissipation of electromagnetic energy in the PVA and its hybrid nanocomposites are revealed by their dielectric loss factor ($\tan\delta_\varepsilon = \varepsilon''/\varepsilon''$) and magnetic loss factor ($\tan\delta_\mu = \mu''/\mu''$) over the same applied frequency. Figure 6a presents $\tan\delta_\varepsilon$ of the PVA/MWCNT−AgNP hybrid nanocomposite, which shows the highest value of 0.70 compared to that of PVA/MWCNT. This is attributed to the energy loss dissipation through the enhanced electrical conduction and slow polarization in the materials when illuminated by the electromagnetic field. While Figure 6b shows that $\tan\delta_\mu$ is high at a low frequency and decreases gradually up to 12 GHz, which is most prominent in the PVA/MWCNT−AgNP hybrid nanocomposite. It could be ascribed to the addition of AgNP with MWCNT, which did not discern strong magnetization in the material, thereby causing high magnetic losses in the X-band frequency.

3.4. Electromagnetic Scattering Analysis. The characteristics of electromagnetic scattering (S-parameters) for all samples have been analyzed in the X-band frequency. Figure 7a,b depicts the variation of the measured power density of reflection (P_{ref}) and absorption (P_{abs}) in relation to the incident power density ($P_{in} = 1$).[33] First, PVA and PVA/MWCNT show a low reflection of the electromagnetic (EM) waves of about 2 and 12%, respectively. The PVA/MWCNT−AgNP hybrid nanocomposite has increased the amount of reflected power up to 35% but gradually drop at 10 GHz onward. However, the EM absorption of PVA and PVA/MWCNT increased about 15 and 40%, respectively. The absorption curves for both materials vary over the applied frequency as a few peaks are observed at 9 and 10 GHz. Remarkably, the PVA/MWCNT−AgNP hybrid nanocomposite shows a significant rise to almost 50% of the absorbed power and the trend is more stable over the frequency range. Most absorption is initiated by free electrons in the MWCNT backbone, and its high surface area can attenuate the wave

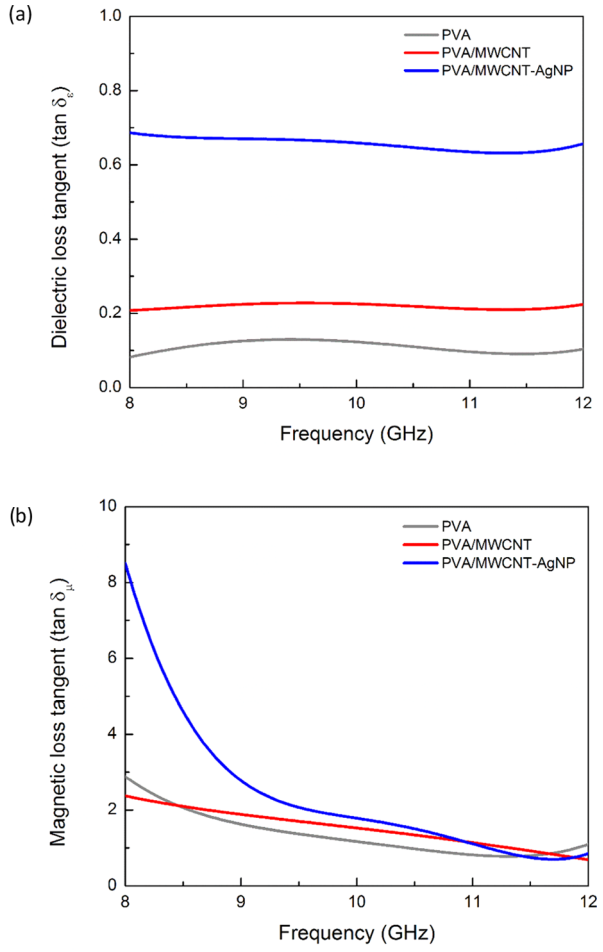

Figure 6. Variation of (a) dielectric loss tangent ($\tan\delta_\varepsilon$) and (b) magnetic loss tangent ($\tan\delta_\mu$) versus frequency in PVA nanocomposites.

energy.[5] The presence of AgNP causes plasmon oscillations when the interaction of metal nanoparticles with EM fields in a dielectric medium can be influenced by the size and shape of nanoparticles.[33] The average size of AgNP ascribed here is 40 nm. In contrast, EM absorption of iron particle nanocomposite was reported in another work only up to 20% with the best size of 50 nm.[34] In addition, the absorption can be triggered by multiple scattering of internal reflections owing to the porous structure of the nanocomposites, as shown earlier by FESEM.[35,36] Multiple internal reflections could take place between MWCNT and AgNP/dielectric matrix interfaces mostly along the crystalline regions. This is because polarization arises from dangling bonds of MWCNT and its defect sites upon the addition of AgNP. This circumstance endows high electric dipoles steering and interfacial polarization in the nanocomposite structure when subjected under an external EM field.[37,38] A general view of the electromagnetic scattering mechanism is illustrated in Figure 8.

Figure 9 shows a comparison of the power data taken at 9 GHz between PVA, PVA/MWCNT, and PVA/MWCNT−AgNP hybrid nanocomposites with an average film thickness of about 0.34 mm. At first sight, PVA demonstrates almost 90% transmission of the incident wave, while PVA/MWCNT just reduces the transmission by 20%. In contrast, the PVA/MWCNT−AgNP hybrid nanocomposite further reduces the transmission by almost 60% compared to PVA/MWCNT. It

https://dx.doi.org/10.1021/acsomega.0c04864
ACS Omega 2021, 6, 4184−4191

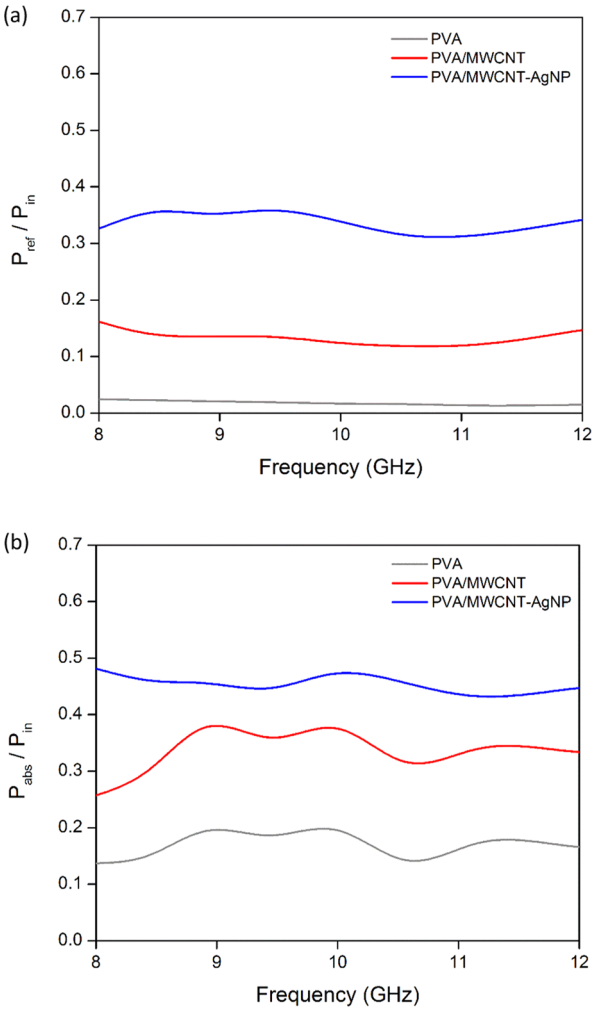

Figure 7. Variation of the (a) reflected power and (b) absorbed power in PVA nanocomposites.

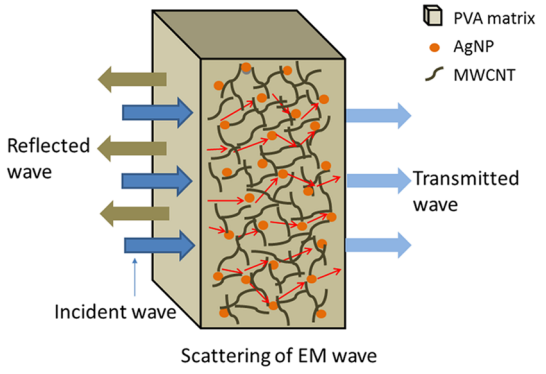

Figure 8. Representation of electromagnetic scattering mechanism in PVA/MWCNT−AgNP.

implies that the addition of AgNP increases the EM absorption of MWCNT and reflection on the surface of the hybrid nanocomposite. This is also corresponding to its favorable dielectric permittivity and ac conductivity in the X-band frequency.

4. CONCLUSIONS

Overall, the incorporation of MWCNT−AgNP as the conductive fillers in the PVA matrix has prompted a hybrid nanocomposite with better functionality than the single component. In this work, the MWCNT−AgNP hybrid was formerly prepared in a single step through the reduction of silver salt ($AgNO_3$) in a dispersion of MWCNT assisted with SDS. Findings have shown superior performance of the PVA/MWCNT−AgNP hybrid nanocomposite prepared through the solution mixing and casting technique. The morphology analysis displayed the conductive pathways formed by an interconnected network of MWCNT−AgNP embedded in the PVA matrix. The electromagnetic characterization of the hybrid nanocomposite in the X-band frequency showed an enhanced permittivity, ε', value of 25 due to the high interfacial polarization between the matrix and both fillers. However, the presence of AgNP with MWCNT did not create strong magnetization in the material, thereby causing higher magnetic losses ($\tan\delta_\mu$) than dielectric losses ($\tan\delta_\varepsilon$) to dissipate the wave energy. Interestingly, it has reduced the amount of transmitted power by almost 60% than that of PVA/MWCNT due to the enhanced absorption and reflection at the surface of the material. The absorption could also be triggered by multiple scattering of internal reflections owing to the porous structure of the nanocomposites. Therefore, it can be potentially suited as a thin film of absorbing material for EM shielding applications.

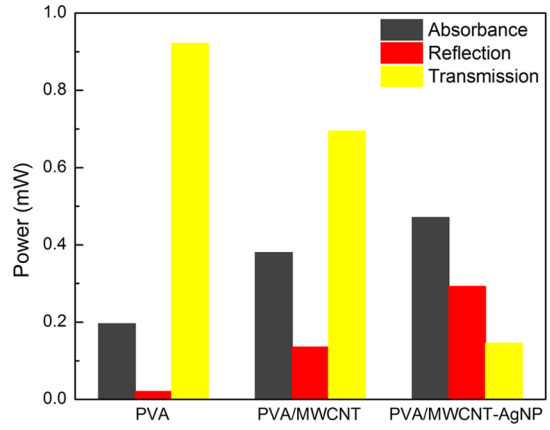

Figure 9. Comparison of power data in PVA nanocomposites taken at 9 GHz.

AUTHOR INFORMATION

Corresponding Authors

Yusliza Yusof − *Nanotechnology and Catalysis Research Center (NANOCAT), University of Malaya, Kuala Lumpur 50603, Malaysia;* orcid.org/0000-0002-9355-2650; Phone: +603-79674509; Email: lyzaa@um.edu.my

Mohd Rafie Johan − *Nanotechnology and Catalysis Research Center (NANOCAT), University of Malaya, Kuala Lumpur 50603, Malaysia*; Phone: +603-79676959; Email: mrafiej@um.edu.my

Authors

Seyedehmaryam Moosavi − *Nanotechnology and Catalysis Research Center (NANOCAT), University of Malaya, Kuala Lumpur 50603, Malaysia;* orcid.org/0000-0003-4441-7302

Irfan Anjum Badruddin − *Research Center for Advanced Materials Science (RCAMS) and Mechanical Engineering Department, College of Engineering, King Khalid University, Abha 61413, Asir, Kingdom Saudi Arabia*

https://dx.doi.org/10.1021/acsomega.0c04864
ACS Omega 2021, 6, 4184−4191

Yasmin Abdul Wahab − *Nanotechnology and Catalysis Research Center (NANOCAT), University of Malaya, Kuala Lumpur 50603, Malaysia*
Nor Aliya Hamizi − *Nanotechnology and Catalysis Research Center (NANOCAT), University of Malaya, Kuala Lumpur 50603, Malaysia*
Marlinda Ab Rahman − *Nanotechnology and Catalysis Research Center (NANOCAT), University of Malaya, Kuala Lumpur 50603, Malaysia*
Sarfaraz Kamangar − *Mechanical Engineering Department, College of Engineering, King Khalid University, Abha 61413, Asir, Kingdom Saudi Arabia*
T. M. Yunus Khan − *Mechanical Engineering Department, College of Engineering, King Khalid University, Abha 61413, Asir, Kingdom Saudi Arabia*

Complete contact information is available at: https://pubs.acs.org/10.1021/acsomega.0c04864

Notes

The authors declare no competing financial interest.

■ ACKNOWLEDGMENTS

The authors extend their appreciation to the Deanship of Scientific Research at King Khalid University for funding this work through the research groups program under grant number (R.G.P 2/74/41). The authors also acknowledge the University of Malaya for providing financial support through NANOCAT RU2020 and BKS002-2020.

■ REFERENCES

(1) Roh, J.-S.; Chi, Y.-S.; Kang, T. J.; Nam, S.-w. Electromagnetic Shielding Effectiveness of Multifunctional Metal Composite Fabrics. *Text. Res. J.* **2008**, *78*, 825−835.
(2) Thomassin, J. M.; Jerome, C.; Pardoen, T.; Bailly, C.; Huynen, I.; Detrembleur, C. Polymer/carbon based composites as electromagnetic interference (EMI) shielding materials. *Mater. Sci. Eng., R* **2013**, *74*, 211−232.
(3) Hussain, S.; Youngs, I. J.; Ford, I. J. The electromagnetic properties of nanoparticle colloids at radio and microwave frequencies. *J. Phys. D: Appl. Phys.* **2007**, *40*, 5331−5337.
(4) Huo, J.; Wang, L.; Yu, H. Polymeric nanocomposites for electromagnetic wave absorption. *J. Mater. Sci.* **2009**, *44*, 3917−3927.
(5) Bhattacharya, P.; Sahoo, S.; Das, C. K. Microwave absorption behaviour of MWCNT based nanocomposites in X-band region. *eXPRESS Polym. Lett.* **2013**, *7*, 212−223.
(6) Al-Saleh, M. H.; Sundararaj, U. Electromagnetic interference shielding mechanisms of CNT/polymer composites. *Carbon* **2009**, *47*, 1738−1746.
(7) Zhang, W.; Xiong, H.; Wang, S.; Li, M.; Gu, Y. Electromagnetic characteristics of carbon nanotube film materials. *Chin. J. Aeronaut.* **2015**, *28*, 1245−1254.
(8) Zhang, D.; Xu, F.; Lin, J.; Yang, Z.; Zhang, M. Electromagnetic characteristics and microwave absorption properties of carbon-encapsulated cobalt nanoparticles in 2-18-GHz frequency range. *Carbon* **2014**, *80*, 103−111.
(9) Dang, Z. M.; Wang, L.; Yin, Y.; Zhang, Q.; Lei, Q. Q. Giant dielectric permittivities in functionalized carbon-nanotube/ electroactive-polymer nanocomposites. *Adv Mater.* **2007**, *19*, 852−857.
(10) Zhen, Y.; Arredondo, J.; Zhao, G. Unusual Dielectric Loss Properties of Carbon Nanotube — Polyvinylidene Fluoride Composites in Low Frequency Region (100 Hz < f < 1 MHz). *Open J. Org. Polym. Mater.* **2013**, *3*, 99−103.
(11) Georgakilas, V.; Gournis, D.; Tzitzios, V.; Pasquato, L.; Guldi, D. M.; Prato, M. Decorating carbon nanotubes with metal or semiconductor nanoparticles. *J. Mater. Chem.* **2007**, *17*, 2679−2694.
(12) Ma, P.-C.; Siddiqui, N. A.; Marom, G.; Kim, J.-K. Dispersion and functionalization of carbon nanotubes for polymer-based nanocomposites: A review. *Composites, Part A* **2010**, *41*, 1345−1367.
(13) Xin, F.; Li, L. Decoration of carbon nanotubes with silver nanoparticles for advanced CNT / polymer nanocomposites. *Composites, Part A* **2011**, *42*, 961−967.
(14) Alimohammadi, F.; Parvinzadeh, M.; Shamei, A.; Kiumarsi, A. Deposition of silver nanoparticles on carbon nanotube by chemical reduction method: Evaluation of surface, thermal and optical properties. *Superlattices Microstruct.* **2012**, *52*, 50−62.
(15) Liang, G. D.; Bao, S. P.; Tjong, S. C. Microstructure and properties of polypropylene composites filled with silver and carbon nanotube nanoparticles prepared by melt-compounding. *Mater. Sci. Eng., B* **2007**, *142*, 55−61.
(16) Lu, J.; Moon, K.-S.; Xu, J.; Wong, C. P. Synthesis and dielectric properties of novel high-K polymer composites containing in-situ formed silver nanoparticles for embedded capacitor applications. *J. Mater. Chem.* **2006**, *16*, 1543−1548.
(17) Lu, J.; Moon, K. S.; Xu, J.; Wong, C. P. In *Dielectric Loss Control Of High-k Polymer Composites By Coulomb Blockade Effects Of Metal Nanoparticles For Embedded Capacitor Applications*, Proceedings International Symposium on Advanced Packaging Materials: Processes, Properties and Interfaces; IEEE, 2005; pp 237−242.
(18) Zhao, W.; Li, M.; Zhang, Z.; Peng, H. International Journal of Smart and Nano Materials EMI shielding effectiveness of silver carbon nanotube sheets. *Int. J. Smart Nano Mater.* **2010**, *1*, 249−260.
(19) Melvin, G. J. H.; Ni, Q. Q.; Natsuki, T.; Wang, Z.; Morimoto, S.; Fujishige, M.; et al. Ag/CNT nanocomposites and their single- and double-layer electromagnetic wave absorption properties. *Synth. Met.* **2015**, *209*, 383−388.
(20) Melvin, G. J. H.; Ni, Q. Q.; Suzuki, Y.; Natsuki, T. Microwave-absorbing properties of silver nanoparticle/carbon nanotube hybrid nanocomposites. *J. Mater. Sci.* **2014**, *49*, 5199−5207.
(21) Van Etten, E. A.; Ximenes, E. S.; Tarasconi, L. T.; Garcia, I. T. S.; Forte, M. M. C.; Boudinov, H. Insulating characteristics of polyvinyl alcohol for integrated electronics. *Thin Solid Films* **2014**, *568*, 111−116.
(22) Bandaru, P. R. Electrical Properties and Applications of Carbon Nanotube Structures. *J. Nanosci. Nanotechnol.* **2007**, *7*, 1239−1267.
(23) Tang, C. M.; Tian, Y. H.; Hsu, S. H. Poly(vinyl alcohol) nanocomposites reinforced with bamboo charcoal nanoparticles: Mineralization behavior and characterization. *Materials* **2015**, *8*, 4895−4911.
(24) Larrude, D. G.; Maia, M. E. H., Jr FLF. Synthesis and Characterization of Silver Nanoparticle-Multiwalled Carbon Nanotube Composites. *J. Nanomater.* **2014**, *654068*, 1−7.
(25) Cullity, B. D. *Elements of X-ray Diffraction*; Addison-Wesley, 1978; p 102.
(26) Chahal, R. P.; Mahendia, S.; Tomar, A. K.; Kumar, S. UV irradiated PVA-Ag nanocomposites for optical applications. *Appl. Surf. Sci.* **2015**, *343*, 160−165.
(27) Mahendia, S.; Tomar, A. K.; Chahal, R. P.; Kumar, S. Synthesis and characterization of silver-poly(vinyl alcohol) nanocomposites. *AIP Conf. Proc.* **2011**, *1349*, 339−340.
(28) Ahmad, Z. Polymeric Dielectric Materials. In *Dielectric Material*; IntechOpen, 2012; pp 1−24.
(29) Bhajantri, R. F.; Ravindrachary, V.; Harisha, A.; Ranganathaiah, C.; Kumaraswamy, G. N. Effect of barium chloride doping on PVA microstructure: Positron annihilation study. *Appl. Phys. A: Mater. Sci. Process.* **2007**, *87*, 797−805.
(30) Groenen, R. Electrical and Microwave Characteristics of Silver Nanoparticle Composites. University of Twente. http://www.utwente.nl/tnw/ims/people/formerMSc/RikGroenen.pdf, 2010.
(31) Yuping, D.; Ma, H.; Shunhua, L.; Xiaodong, C.; Huifeng, C.; Duan, Y.; et al. Absorbing properties of α-manganese dioxide/carbon black double-layer composites. *J. Phys. D: Appl. Phys.* **2008**, *41*, No. 125403.

(32) Zhao, T.; Hou, C.; Zhang, H.; Zhu, R.; She, S.; Wang, J.; et al. Electromagnetic wave absorbing properties of amorphous carbon nanotubes. *Sci. Rep.* **2014**, *4*, No. 5619.
(33) Kelly, K. L.; Coronado, E.; Zhao, L. L.; Schatz, G. C. The Optical Properties of Metal Nanoparticles: The Influence of Size, Shape, and Dielectric Environment. *J. Phys. Chem. B* **2003**, *107*, 668−677.
(34) Jalali, M.; Dauterstedt, S.; Michaud, A.; Wuthrich, R. Electromagnetic shielding of polymer − matrix composites with metallic nanoparticles. *Composites, Part B* **2011**, *42*, 1420−1426.
(35) Saini, P.; Choudhary, V. Enhanced electromagnetic interference shielding effectiveness of polyaniline functionalized carbon nanotubes filled polystyrene composites. *J. Nanopart. Res.* **2013**, *15*, 1−7.
(36) Al-ghamdi, A. A.; El-tantawy, F. New electromagnetic wave shielding effectiveness at microwave frequency of polyvinyl chloride reinforced graphite / copper nanoparticles. *Composites, Part A* **2010**, *41*, 1693−1701.
(37) Vázquez, E.; Prato, M. Carbon Nanotubes and Microwaves: Interactions, Responses, and Applications. *ACS Nano* **2009**, *3*, 3819−3824.
(38) Zhang, D.; Hao, Z.; Qian, Y.; Huang, Y.; Bizeng; Yang, Z.; et al. Simulation and measurement of optimized microwave reflectivity for carbon nanotube absorber by controlling electromagnetic factors. *Sci. Rep.* **2017**, *7*, No. 479.

https://dx.doi.org/10.1021/acsomega.0c04864
ACS Omega 2021, 6, 4184−4191